J|A|C|S
ARTICLES
Published on Web 05/01/2007

Porphyrin-Diones and Porphyrin-Tetraones: Reversible Redox Units Being Localized within the Porphyrin Macrocycle and Their Effect on Tautomerism

Karl M. Kadish,*,† Wenbo E,† Riqiang Zhan,† Tony Khoury,‡ Linda J. Govenlock,‡ Jognandan K. Prashar,‡ Paul J. Sintic,‡ Kei Ohkubo,§ Shunichi Fukuzumi,*,§ and Maxwell J. Crossley*,‡

Contribution from the Department of Chemistry, University of Houston, Houston, Texas 77204-5003, School of Chemistry, The University of Sydney, NSW 2006, Australia, and Department of Material and Life Science, Graduate School of Engineering, Osaka University, SORST, Japan Science and Technology Agency (JST), Suita, Osaka 565-0871, Japan

Received February 2, 2007; E-mail: kkadish@uh.edu; fukuzumi@chem.eng.osaka-u.ac.jp; m.crossley@chem.usyd.edu.au

Abstract: Porphyrin-2,3-diones and porphyrin-2,3,7,8- and porphyrin-2,3,12,13-tetraones were shown to have a redox-active unit that can function independently of the macrocycle at large. Electroreduction of 5,10,15,20-tetrakis(3,5-di-*tert*-butylphenyl)porphyrin-2,3-diones [(P-dione)M] and the corresponding -2,3,-12,13-tetraones [L-(P-tetraone)M] and -2,3,7,8-tetraones [C-(P-tetraone)M], where M = 2H, Cu^{II}, Zn^{II}, Ni^{II}, and Pd^{II} was investigated and the products were characterized by ESR and thin-layer UV−visible spectroelectrochemistry. Electrochemical and spectroelectrochemical data show that the first two reductions of the porphyrin-diones and the first three reductions of the porphyrin-tetraones occur at the dione units. This was confirmed by ESR spectra of first reduction products which show that the electron spin is totally localized on a semidione unit, independent of the central metal ion and of the number and location of dione units. ESR spectra of the radical anions derived from free-base porphyrin-2,3-dione [(P-dione)2H] and porphyrin-2,3,12,13-tetraone [L-(P-tetraone)2H] confirm the *trans*-arrangement of the two inner protons and their location on nonsubstituted pyrrolic rings, thereby maintaining an 18-atom 18-π electron bacteriochlorin-like aromatic delocalization pathway. The redox unit is not similarly isolated in the corner free-base porphyrin-2,3,7,8-tetraone [C-(P-tetraone)2H]. A one-electron reduction of C-(P-tetraone)2H leads to the formation of a tautomer with *trans* inner hydrogens with one residing on the N of the ring with the reduced unit as the only detectable product. This process is favorable because it creates a more delocalized 18-atom 18-π electron aromatic pathway. This result is consistent with the measured redox potentials which show the first reduction of C-(P-tetraone)2H to be substantially easier than (P-dione)2H or L-(P-tetraone)2H.

Introduction

Porphyrins have a highly delocalized π system that is suitable for efficient electron-transfer reactions.[1,2] Rich and extensive absorption features of porphyrins guarantee increased absorption cross sections and an efficient use of the solar spectrum.[1,2] The excited states of porphyrins can act as both electron donors and electron acceptors in photoinduced electron-transfer reactions to produce radical cations and radical anions, respectively.[2,3] Extensive efforts have been made to alter the redox potentials and electron-transfer reactivities by introducing electron-donating or -withdrawing substituents on the porphyrin ring for easier oxidation or reduction.[4−7] In all cases, however, the substituents are simply modulating the redox chemistry of the porphyrin macrocycle. This study seeks to incorporate electroactive functionality into the porphyrin structure that can function independently of the macrocycle. Such porphyrin systems with independent redox sites might have applications in electron-transfer reactions and molecular electronics and could make possible further chemical reactions at the second site that would modify such properties like metal ion coordination. In this work we investigate α-dione units for this purpose.

† University of Houston.
‡ The University of Sydney.
§ Osaka University.

(1) Fukuzumi, S. In *The Porphyrin Handbook*; Kadish, K. M., Smith, K., Guilard, R., Eds.; Academic Press: San Diego, CA; 2000; Vol. 8, p 115.
(2) Gust, D.; Moore, T. A. In *The Porphyrin Handbook*; Kadish, K. M., Smith, K. M., Guilard, R., Eds.; Academic Press: New York, 2000; Vol. 8, p 153.
(3) Fukuzumi, S.; Imahori, H. In *Electron Transfer in Chemistry*; Balzani, V., Ed.; Wiley-VCH: Weinheim, 2001; Vol. 2, p 927.
(4) Kadish, K. M. *Prog. Inorg. Chem.* **1986**, *34*, 435.
(5) Kadish, K. M.; Royal, G.; Caemelbeck, E. V.; Gueletti, L. In *The Porphyrin Handbook*; Kadish, K. M., Smith, K. M., Guilard, R., Eds.; Academic Press: New York, 2000; Vol. 9, p 59.
(6) (a) Wijesekera, T.; Matsumoto, A.; Dolphin, D.; Lexa, D. *Angew. Chem., Int. Ed. Engl.* **1990**, *29*, 1028. (b) Ozette, K.; Leduc, P.; Palacio, M.; Bartoli, J.-F.; Barkigia, K. M.; Fajer, J.; Battioni, P.; Mansuy, D. *J. Am. Chem. Soc.* **1997**, *119*, 6442. (c) Palacio, M.; Juillard, A.; Leduc, P.; Battioni, P.; Mansuy, D. *J. Organomet. Chem.* **2002**, *643*−*644*, 522.
(7) (a) Teraxono, Y.; Patrick, B. O.; Dolphin, D. H. *Inorg. Chem.* **2002**, *41*, 6703. (b) Bhyrappa, P.; Sankar, M.; Varghese, B. *Inorg. Chem.* **2006**, *45*, 4136.

10.1021/ja070759b CCC: $37.00

Cyclic ketones and quinones have carbonyl groups in which the carbonyl carbons are both part of the functional group and part of the ring structure. Electrochemical properties of numerous diones and 1,2-quinones and ESR characterization of the related semidiones, their one-electron reduction product, have been extensively studied.[8−12] The only macrocycles similar to a porphyrin to have been investigated were 5,15-dioxoporphodimethenes in which the oxo groups are on opposite meso-positions, akin to an 18- or 22-atom *p*-quinone, thereby disrupting the macrocyclic π-electron conjugation. Reduction of these compounds, however, involves the macrocycle.[13]

Porphyrin-2,3-diones,[14−15] porphyrin-2,3,7,8-tetraones, and porphyrin-2,3,12,13-tetraones,[16−17] which contain α-dione units across β,β'-pyrrolic positions on the porphyrin periphery, are versatile building blocks for the synthesis of laterally extended porphyrin arrays based on linear and square grid architectures by annulation reactions involving the α-dione units.[14−48] Reaction of porphyrin-2,3-diones with 1,2-diamino-arenes gives ring-fused quinoxalino[2,3-*b*]porphyrins,[14−46] while reaction with ammonium acetate and aldehydes gives imidazolo[4,5-*b*]porphyrins.[47,48] Use of 1,2,4,5-arenetetramines or dialdehydes in these reactions allows synthesis of corresponding linked bisporphyrins.[17,18,29,30,32,33,37,39,44] Similar reactions of the porphyrin-tetraones give linearly annulated diquinoxalinoporphyrins and diimidazoloporphyrins[16,47] and, when 1,2,4,5-arenetetramines are used, laterally extended porphyrin-based oligomers,[16,18,19,31,43,46] an example being a conjugated planar tetrakis-porphyrin that spans 6.5 nm which provides for the development of new classes of organic materials for molecular wires.[16,19,49−53] The dione functionality can be transformed into other units to give ring-expanded and ring-contracted porphyrin systems.[14,54]

There is no reported data in the literature on the redox properties of porphyrin-α-diones and porphyrin-tetraones, and nothing is therefore known about the potentials for their electroreduction or degree of delocalization of the added electron. Reduction of the electroactive dione units should lead first to a semidione radical anion. These semidione radical anions have an increased double bond character between the carbonyl carbon atoms relative to diones.[11] There are two possible fates for the newly generated carbon−carbon electron density; it can become part of an aromaticity of the macrocyclic ring in a fashion similar to that seen in the one-electron reduction of *ortho*-quinones which leads to an aromatic semiquinone radical anion, or it might function as the isolated semidione radical anion in which aromaticity of the rest of the macrocycle is maintained in a chlorin- or bacteriochlorin-like delocalization pathway.

This paper reports the electrochemistry and spectroelectrochemistry of porphyrin-diones and porphyrin-tetraones that exhibit unique redox properties in that they have a redox-active dione unit that can function independently of the macrocycle. The investigated complexes are shown in Chart 1. The 15 compounds can be divided into three distinct structural types: porphyrin-2,3-diones [(P-dione)M **2a**−**e**], linear porphyrin-2,3,-12,13-tetraones [L-(P-tetraone)M **3a**−**e**], and corner porphyrin-2,3,7,8-tetraones [C-(P-tetraone)M **4a**−**e**], where P is 5,10,15,-20-tetrakis(3,5-di-*tert*-butylphenyl)porphyrin and M = 2H, Cu^{II}, Zn^{II}, Ni^{II}, and Pd^{II}, **a**−**e**, respectively.

A comparison of the properties of porphyrin-diones **2a**−**e** and porphyrin-tetraones **3a**−**e** and **4a**−**e** with those of the parent porphyrin and its metalated derivatives [(P)M **1a**−**e**] is made and shows that initial redox reactions occur at the dione units and are largely independent of the rest of the macrocycle, including the central metal ion and number and location of the

(8) Heineman, W. R.; Burnett, J. N.; Murray, R. W. *Anal. Chem.* **1968**, *40*, 1974.
(9) Dirlam, J. P.; Winstein, S. *J. Org. Chem.* **1971**, *36*, 1559.
(10) Rubin, M. B.; Ben-Bassat, J. M. *Tetrahedron Lett.* **1971**, *37*, 3403.
(11) (a) Russell, G. A.; Bruni, P. *Tetrahedron* **1970**, *26*, 3449. (b) Russell, G. A.; Gerlock, J. L.; Lawson, D. F. *J. Am. Chem. Soc.* **1971**, *93*, 4088.
(12) Elson, I. H.; Kemp, T. J.; Greatorex, D.; Jenkins, H. D. B. *J. Chem. Soc., Faraday Trans. 2* **1973**, *69*, 665.
(13) (a) Barnett, G. H.; Evans, B.; Smith, K. M. *Tetrahedron* **1975**, *31*, 2711. (b) Fuhrhop, J. H.; Baumgartner, E.; Bauer, H. *J. Am. Chem. Soc*. **1981**, *103*, 5854. (c) Balch, A. L.; Noll, B. C.; Phillips, S. L.; Reid, S. M.; Zovinka, E. P. *Inorg. Chem*. **1993**, *32*, 4730. (d) Balch, A. L.; Noll, B. C.; Olmstead, M. M.; Phillips, S. L. *Inorg. Chem*. **1996**, *35*, 6495. (e) Khoury, R. G.; Jaquinod, L.; Nurco, D. J.; Smith, K. M. *Chem. Commun.* **1996**, 1143.
(14) Crossley, M. J.; King, L. G. *J. Chem. Soc., Chem. Commun.* **1984**, 920.
(15) Crossley, M. J.; Burn, P. L.; Langford, S. J.; Pyke, S. M.; Stark, A. G. *J. Chem. Soc., Chem. Commun.* **1991**, 1567.
(16) Crossley, M. J.; Govenlock, L. J.; Prashar, J. K. *J. Chem. Soc., Chem. Commun.* **1995**, 2379.
(17) Promarak, V.; Burn, P. *J. Chem. Soc., Perkin Trans. 1* **2001**, 14.
(18) Crossley, M. J.; Burn, P. L. *Chem. Commun.* **1987**, 39.
(19) Crossley, M. J.; Burn, P. L. *J. Chem. Soc., Chem. Commun.* **1991**, 1569.
(20) Crossley, M. J.; King, L. G.; Newsom, I. A.; Sheehan, C. S. *J. Chem. Soc., Perkin Trans. 1* **1996**, 2675.
(21) Atkinson, E. J.; Oliver, A. M.; Paddon-Row, M. N. *Tetrahedron Lett.* **1993**, *34*, 6147.
(22) Crossley, M. J.; Burn, P. L.; Langford, S. J.; Prashar, J. K. *J. Chem. Soc., Chem. Commun.* **1995**, 1921.
(23) Crossley, M. J.; Try, A. C.; Walton, R. *Tetrahedron Lett.* **1996**, *37*, 6807.
(24) Crossley, M. J.; Prashar, J. K. *Tetrahedron Lett.* **1997**, *38*, 6751.
(25) Reek, J. N. H.; Rowan, A. E.; de Gelder, R.; Beurskens, P. T.; Crossley, M. J.; De Feyter, S.; de Schryver, F.; Nolte, R. J. M. *Angew. Chem., Int. Ed.* **1997**, *36*, 361.
(26) Johnston, M. R.; Warrener, R. N.; Gunter, M. J. *Chem. Commun.* **1998**, 2739.
(27) Reek, J. N. H.; Schenning, A. P. H. J.; Bosman, A. W.; Meijer, E. W.; Crossley, M. J. *Chem. Commun.* **1998**, 11.
(28) Reek, J. N. H.; Rowan, A. E.; Crossley, M. J.; Nolte, R. J. M. *J. Org. Chem.* **1999**, *64*, 6653.
(29) Beavington, R.; Burn, P. L. *J. Chem. Soc., Perkin Trans. 1* **2000**, 1231.
(30) Beavington, R.; Burn, P. L. *J. Chem. Soc., Perkin Trans. 1* **2000**, 605.
(31) Yeow, E. K. L.; Sintic, P. J.; Cabral, N. M.; Reek, J. N. H.; Crossley, M. J.; Ghiggino, K. P. *Phys. Chem. Chem. Phys.* **2000**, *2*, 4281.
(32) Flamigni, L.; Marconi, G.; Johnston, M. R. *Phys. Chem. Chem. Phys.* **2001**, *3*, 4488.
(33) Crossley, M. J.; Johnston, L. A. *Chem. Commun.* **2002**, 1122.
(34) Crossley, M. J.; Thordarson, P. *Angew. Chem., Int. Ed.* **2002**, *41*, 1709.
(35) Flamigni, L.; Talarico, A. M.; Barigelletti, F.; Johnston, M. R. *Photochem. Photobiol. Sci.* **2002**, *1*, 190.
(36) Johnston, M. R.; Gunter, M. J.; Warrener, R. N. *Tetrahedron* **2002**, *58*, 3445.
(37) Johnston, M. R.; Latter, M. J. *J. Porphyrins Phthalocyanines* **2002**, *6*, 757.
(38) Johnston, M. R.; Latter, M. J.; Warrener, R. N. *Org. Lett.* **2002**, *4*, 2165.
(39) Sendt, K.; Johnston, L. A.; Hough, W. A.; Crossley, M. J.; Hush, N. S.; Reimers, J. R. *J. Am. Chem. Soc.* **2002**, *124*, 9299.
(40) Crossley, M. J.; Sintic, P. J.; Walton, R.; Reimers, J. R. *Org. Biomol. Chem.* **2003**, *1*, 2777.
(41) Thordarson, P.; Marquis, A.; Crossley, M. J. *Org. Biomol. Chem.* **2003**, *1*, 1216.
(42) Warrener, R. N.; Sun, H.; Johnston, M. R. *Aust. J. Chem.* **2003**, *56*, 269.
(43) Crossley, M. J.; Sintic, P. J.; Hutchison, J. A.; Ghiggino, K. P. *Org. Biomol. Chem.* **2005**, *3*, 852.
(44) Armstrong, R. S.; Foran, G. J.; Hough, W. A.; D'Alessandro, D. M.; Lay, P. A.; Crossley, M. J. *Dalton Trans.* **2006**, 4805.
(45) Gaynor, S. P.; Gunter, M. J.; Johnston, M. R.; Warrener, R. N. *Org. Biomol. Chem.* **2006**, *4*, 2253.
(46) Ohkubo, K.; Sintic, P. J.; Tkachenko, N. V.; Lemmetyinen, H.; E, W.; Ou, Z.; Shao, J.; Kadish, K. M.; Crossley, M. J.; Fukuzumi, S. *Chem. Phys.* **2006**, *326*, 3.
(47) Crossley, M. J.; McDonald, J. A. *J. Chem. Soc., Perkin Trans. 1* **1999**, 242.
(48) Kashiwagi, Y.; Ohkubo, K.; McDonald, J. A.; Blake, I. M.; Crossley, M. J.; Araki, Y.; Ito, O.; Imahori, H.; Fukuzumi, S. *Org. Lett.* **2003**, *5*, 2719.
(49) Hush, N. S.; Reimers, J. R.; Hall, L. E.; Johnston, L. A.; Crossley, M. J. *Ann. N.Y. Acad. Sci.* **1998**, *852*, 1.
(50) Anderson, H. L. *Chem. Commun.* **1999**, 2323.
(51) Reimers, J. R.; Hall, L. E.; Crossley, M. J.; Hush, N. S. *J. Phys. Chem. A* **1999**, *103*, 4385.
(52) Reimers, J. R.; Hush, N. S.; Crossley, M. J. *J. Porphyrins Phthalocyanines* **2002**, *6*, 795.
(53) Reimers, J. R.; Bilic, A.; Cai, Z. -L.; Dahlbom, M.; Lambropoulos, N. A.; Solomon, G. C.; Crossley, M. J.; Hush, N. S. *Aust. J. Chem.* **2004**, *57*, 1133.
(54) Crossley, M. J.; Hambley, T. W.; King, L. G. *Bull. Soc. Chim. Fr.* **1996**, *133*, 735.

Chart 1

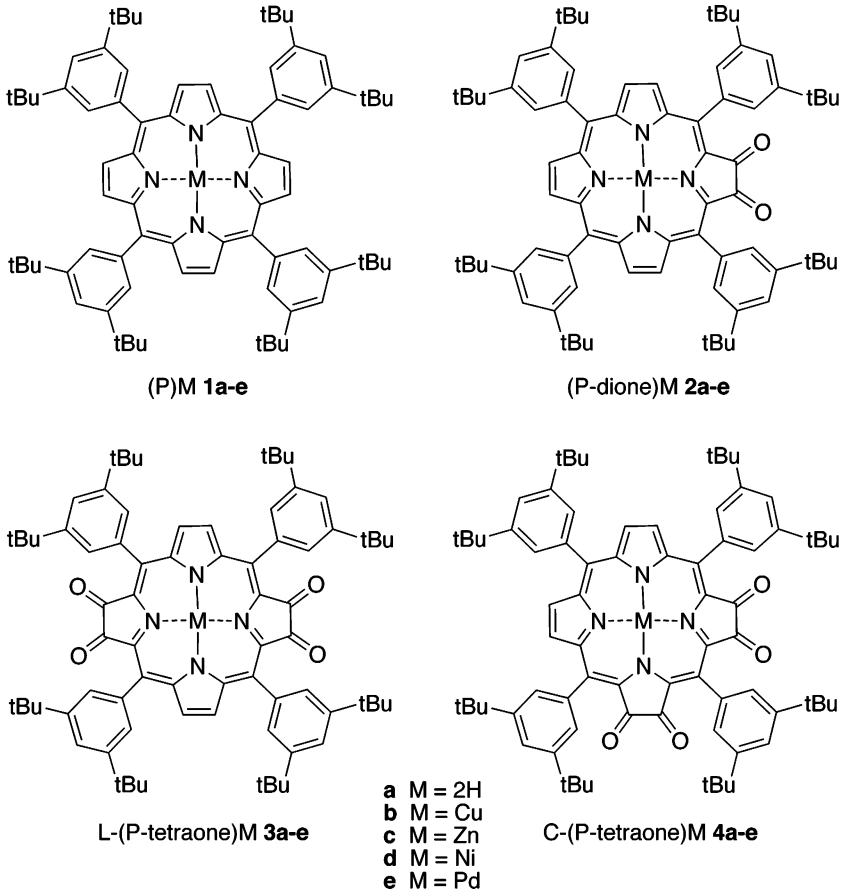

dione units, the only exception being in the case of the free-base corner porphyrin-2,3,7,8-tetraone **4a**. In the other two free-base cases, **2a** and **3a**, the semidione unit serves to lock tautomerism to the tautomer that allows the reduced unit to stay separate from the rest of the macrocycle.

Results and Discussion

Synthesis of Metalloporphyrins. The metalloporphyrins **2b**−**e**, **3b**−**e**, and **4b**−**e** were prepared from the free-base porphyrin-dione[18] **2a**, free-base linear porphyrin-tetraone[16] **3a**, and free-base corner porphyrin-tetraone[16] **4a**, respectively. These reaction conditions are optimized and afford the desired products in high yield and fast reaction times. This has been achieved by using high boiling point solvents which help solubilize both the porphyrins and the metal(II) salt.

Electrochemistry of (P-dione)M 2b-e and (P-dione)2H 2a. The electrochemistry of each porphyrin-dione **2a**−**e** was examined in both CH_2Cl_2 and PhCN containing 0.1 M TBAP. The initial reductions of all compounds are reversible in both solvents, and the site of electron transfer could be determined by UV−visible and/or ESR characterization of the singly and doubly reduced products (*vide infra*). Table 1 contains the $E_{1/2}$ values of the porphyrin-diones **2a**−**e** in CH_2Cl_2 and summarizes also the number of electrons transferred in each oxidation, which was either one or two, and the potential separations between the first three reductions of compounds labeled as Δ_{2-1} and Δ_{3-2}.[56] Typical cyclic voltammograms for the (P-dione)Cu **2b** and free base (P-dione)2H **2a** in CH_2Cl_2 are shown in Figure 1.[57]

The electrochemistry of free-base and metallo-5,10,15,20-tetraarylporphyrins in nonaqueous media has been well characterized in the literature.[58] The free-base and metalated porphyrins **1a**−**e** were expected to undergo well-separated one-electron oxidations and one-electron reductions at the porphyrin π-ring system, and this is indeed what was observed. For example, (P)Cu **1b** in CH_2Cl_2 containing 0.10 M TBAP is reduced at $E_{1/2} = -1.36$ V and $E_p = -1.88$ V and oxidized at $E_{1/2} = 0.94$ and 1.23 V as shown in Figure 1a. The potential separation between the reversible first oxidation and reversible first reduction (the electrochemical HOMO−LUMO gap) amounts to 2.30 V, and the absolute potential differences between the two reductions and two oxidations of (P)Cu **1b** in PhCN[55] amount to 0.52 V for reduction and 0.29 V for oxidation. The same type of redox behavior is also seen for the free-base porphyrin (P)2H **1a** in CH_2Cl_2 (Figure 1c).

Quite different redox behavior from that of (P)Cu **1b** and (P)2H **1a**, reported above, is seen for (P-dione)Cu **2b** and (P-dione)2H **2a**. The difference between the electrochemistry of the two types of macrocycles is striking. The two one-electron oxidations of the porphyrin-diones **2a** and **2b** to generate π-cation radicals and π-dications in CH_2Cl_2 are not separated

(55) Ou, Z. E. W.; Shao, J.; Burn, P. L.; Sheehan, C. S.; Walton, R.; Kadish, K. M.; Crossley, M. J. *J. Porphyrins Phthalocyanines* **2005**, *9*, 142.
(56) For the values obtained using PhCN as solvent, see Supporting Information Table S1.
(57) For cyclic voltammograms of (P-dione)Zn **2c**, (P-dione)Ni **2d**, and (P-dione)Pd **2e**, see Supporting Information S3.
(58) Kadish, K. M.; Caemelbecke, V.; Royal, G. The Porphyrin Handbook. In *The Porphyrin Handbook*; Kadish, K. M., Smith, K. M., Guilard, R., Eds.; Academic Press: San Diego, 2000; Vol. 8, pp 1−114.

Table 1. Half-Wave Potentials (V vs SCE) of Porphyrin-Diones and -Tetraones in CH_2Cl_2, 0.1 M TBAP[a]

	oxidation		reduction					
compound	second	first	first	second	third	fourth	Δ_{2-1}[b]	Δ_{3-2}[c]
(P)2H[d] **1a**		0.95 (1e)	−1.22	−1.55				
(P)Cu **1b**	1.23 (1e)	0.94 (1e)	−1.36	−1.88[e]				
(P)Zn[d] **1c**	1.06 (1e)	0.72 (1e)	−1.42					
(P)Ni[d] **1d**		0.93 (2e)	−1.31					
(P)Pd[d] **1e**	1.52[e] (1e)	1.05 (1e)	−1.32	−1.95[e]				
(P-dione)2H **2a**		1.06 (2e)	−0.59	−0.95	−1.86[e]		0.36	0.91
(P-dione)Cu **2b**		1.10 (2e)	−0.49	−1.21	−1.62		0.72	0.41
(P-dione)Zn **2c**	1.00 (1e)	0.85 (1e)	−0.57	−1.25[e]	−1.68		0.68	0.43
(P-dione)Ni **2d**		1.17 (2e)	−0.51	−1.24	−1.61		0.73	0.37
(P-dione)Pd **2e**	1.44 (1e)	1.19 (1e)	−0.50	−1.26	−1.61		0.76	0.35
L-(P-tetraone)2H **3a**		1.09 (2e)	−0.47	−0.72[e]	−1.01	−1.80	0.25	0.29
L-(P-tetraone)Cu **3b**		1.11 (2e)	−0.26	−0.70	−1.34[e]	−1.85	0.44	0.64
L-(P-tetraone)Zn **3c**		0.95 (2e)	−0.34	−0.73	−1.36[e]	−1.84	0.39	0.63
L-(P-tetraone)Ni **3d**		1.20 (2e)	−0.25	−0.68	−1.38	−1.84	0.43	0.70
L-(P-tetraone)Pd **3e**	1.49 (1e)	1.29 (1e)	−0.29	−0.64	−1.34[e]	−1.81	0.35	0.70
C-(P-tetraone)2H **4a**		1.06 (2e)	−0.28	−0.79	−1.09[f]	−1.90[e]	0.51	0.30
C-(P-tetraone)Cu **4b**		1.16[e] (2e)	−0.33[g]	−0.67	−1.37[e]		0.34	0.70
C-(P-tetraone)Zn **4c**		0.96 (2e)	−0.46	−0.76	−1.47[e]		0.30	0.71
C-(P-tetraone)Ni **4d**		1.22 (2e)	−0.32	−0.69	−1.62[e]		0.37	0.93
C-(P-tetraone)Pd **4e**		1.29 (1e)	−0.33	−0.69	−1.46[e]		0.36	0.77

[a] All potentials are good to ±10 mV. [b] Difference between the first and second reduction potentials. [c] Difference between the second and third reduction potentials. [d] Data taken from ref 55. [e] Peak potential at a scan rate of 0.1 V/s for irreversible reaction. [f] Unknown irreversible reduction is also observed at $E_p = -1.60$ V at a scan rate of 0.1 V/s. [g] Unknown irreversible reduction is also observed at $E_p = -0.46$ V at a scan rate of 0.1 V/s.

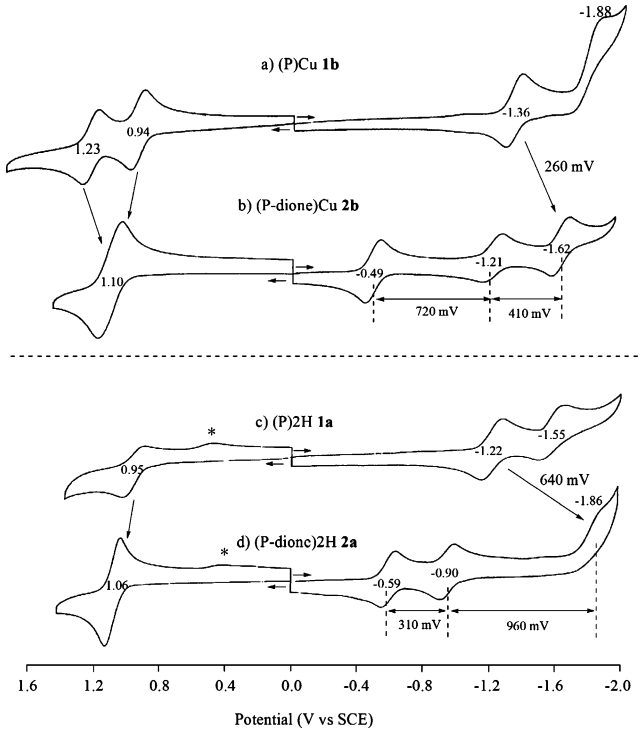

Figure 1. Cyclic voltammograms of (a) (P)Cu **1b**, (b) (P-dione)Cu **2b**, (c) (P)2H **1a**, and (d) (P-dione)2H **2a** in CH_2Cl_2, 0.1 M TBAP. The asterisk * indicates the irreversible cathodic peak due to reduction of an isoporphyrin formed from the dication in solution.

in potential as in the case of (P)Cu **1b** ($E_{1/2} = 0.94$ and 1.23 V) but are instead overlapped in potential, thus giving an apparent one-step conversion of the neutral compound to its doubly oxidized dicationic form (Figure 1b). These processes occur at $E_{1/2} = 1.10$ V for (P-dione)Cu **2b** (Figure 1b) and 1.06 V for (P-dione)2H **2a** (Figure 1d), both values being shifted in a positive direction from the first one-electron oxidation of (P)-Cu **1b** and (P)2H **1a** by 160 and 110 mV, respectively. The positive shift in $E_{1/2}$ for oxidation of the porphyrin-diones is consistent with the electron-withdrawing nature of the oxo groups which make the porphyrin ring more electropositive, hence leading to a more difficult oxidation.

On the other hand, the overlapped second oxidation of (P-dione)Cu **2b** is shifted negatively by 130 mV as compared to (P)Cu **1b** in CH_2Cl_2 indicating a strong ion pairing of the doubly oxidized Cu(II) porphyrin-dione. This is rarely observed in the case of simple metalloporphyins having tetraphenylporphyrin (TPP) or octaethylporphyrin (OEP)-like structures,[58] and, with the single exception of Ni(II) derivatives,[59−61] is almost never observed for any other porphyrin in a solvent such as CH_2Cl_2. A negative shift in $E_{1/2}$ is also observed for the second oxidation of (P-dione)2H **2a** (leading to an overlapping two-electron oxidation), although the magnitude of the potential shift cannot be ascertained in CH_2Cl_2 due to the coupled chemical reaction following formation of the highly reactive π-cation radical of (P)2H **1a** (see irreversible redox couple in Figure 1c).

Porphyrin-diones **2a**−**e** differ significantly from the unsubstituted porphyrins (P)M **1a**−**e** in their reductions where three one-electron additions are observed for each of the porphyrin-diones. The first reduction of the five investigated porphyrin-diones, (P-dione)M **2a-e**, is located in a range of $E_{1/2}$ values between −0.49 and −0.59 V vs SCE in CH_2Cl_2 (Table 1), and between −0.44 and −0.57 V vs SCE in PhCN,[56] and is thus only slightly dependent upon solvent. The second one-electron reduction of the porphyrin-diones ranges between $E_{1/2}$ values of −1.21 and −1.26 V for the metalated complexes **2b**−**e** but is significantly easier for the free-base porphyrin-dione **2a**, $E_{1/2}$ being −0.95 V in CH_2Cl_2. Finally the third reduction of the metalated porphyrin-diones **2b**−**e** spans a narrow $E_{1/2}$ range of

(59) Chang, D.; Malinski, T.; Ulman, A.; Kadish, K. M. *Inorg. Chem.* **1984**, *23*, 817−824.
(60) Kadish, K. M.; Lin, M.; Van Caemelbecke, E.; De Stefano, G.; Medforth, C. J.; Nurco, D. J.; Nelson, N. Y.; Krattinger, B.; Muzzi, C. M.; Jaquinod, L.; Xu, Y.; Shyr, D. C.; Smith, K. M.; Shelnutt, J. A. *Inorg. Chem.* **2002**, *41*, 6673.
(61) Ghosh, A.; Halvorsen, I.; Nilsen, H. J.; Steene, E.; Wondigagegn, T.; Lie, R.; van Caemelbecke, E.; Guo, N.; Qu, Z.; Kadish, K. M. *J. Phys. Chem. B* **2001**, *105*, 8120.

Scheme 1

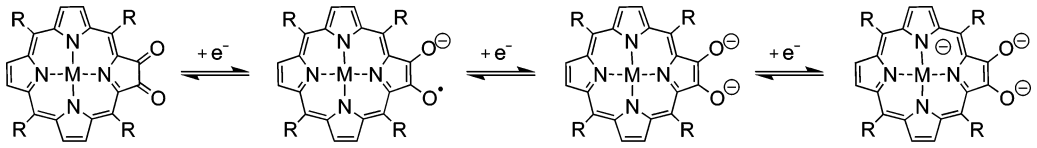

R = 3,5-di-*tert*-butylphenyl

−1.61 to −1.68 V, while the porphyrin-dione **2a** is irreversibly reduced at more negative potentials; the measured $E_p = -1.86$ V in CH_2Cl_2 for a scan rate of 0.1 V/s. Almost identical values are obtained for the same processes using PhCN as solvent.[56]

The electrochemistry of the other three (P-dione)M derivatives, where M = Zn, Ni, Pd, **2c**−**e** is similar to that of (P-dione)Cu **2b** in the two solvents (see Tables 1 and Supporting Information S2). Addition of the first electron to the (P-dione)M **2** is significantly easier in each case than reduction of the analogous (P)M **1** compound with the same metal ion. The absolute difference in half-wave potentials between the first reductions in the two series of compounds ranges from 800 to 850 mV in CH_2Cl_2. The second reduction of (P-dione)M **2** to give $[(P\text{-dione})M]^{2-}$ is also easier than the second reduction of the analogous (P)M complex **1**, and both of these results are consistent with the addition of two electrons to the oxo groups of the dione prior to reduction of the conjugated macrocycle at more negative potentials.

The relevant electrode reactions of (P-dione)M are given in Scheme 1 and are confirmed by thin-layer spectroelectrochemical and ESR data (*vide infra*). Prior to discussion of this data, however, it is important to point out key differences in $E_{1/2}$ values between the second and third reductions of the four metalloporphyrin-diones (P-dione)M **2b**−**e** as compared to the same reactions of the free-base derivative, (P-dione)2H **2a**. The formation of doubly reduced $[(P\text{-dione})2H]^{2-}$ at $E_{1/2} = -0.95$ V in CH_2Cl_2 and at −0.98 V in PhCN is easier than formation of doubly reduced $[(P\text{-dione})M]^{2-}$ by more than 250 mV in the same solvents, but conversely, the formation of triply reduced $[(P\text{-dione})2H]^{3-}$ at $E_p = -1.86$ to −1.92 V is harder by a similar amount than formation of triply reduced $[(P\text{-dione})M]^{3-}$ under the same solution conditions. This is illustrated graphically in Figure 1 and Supporting Information Figure S3 where the difference between $\Delta E_{1/2}$ values for the stepwise reductions in CH_2Cl_2 are indicated on the voltammograms. The differences range from 680 to 760 and 370−410 mV in the case of (P-dione)M **2b-e** as compared to 360 and 910 mV in the case of (P-dione)2H **2a**.

Clearly differences exist between the metalated porphyrin-diones and nonmetalated (P-dione)2H **2a** in relative stabilities of the reduced species and the driving force for reduction. The much easier second reduction of (P-dione)2H **2a** as compared to (P-dione)M **2b**−**e** can be accounted for by a transmission of some electron density from the oxygens to the porphyrin macrocycle of the doubly reduced species and, if this occurred, should also lead to a harder third reduction of (P-dione)2H **2a** as compared to the metalated porphyrins, which is what is experimentally observed. The source of these differences is described below. Differences in the site of electron transfer or electron distribution between the reduced forms of (P-dione)-Cu **2b** and (P-dione)2H **2a** should be evident in UV−visible and ESR spectra of the species generated electrochemically or chemically, and this data is now presented.

Site of Electron Addition to (P-dione)M 2 and (P-dione)-2H 2a. The site of electron addition to the (P-dione)M **2b**−**e** and (P-dione)2H **2a** was first examined by thin-layer spectroelectrochemistry. UV−visible spectra were obtained during the first two reductions of each compound or during all three reductions in some cases, an example of which is given in Figure 2 for the stepwise one-electron additions to (P-dione)Cu **2b** in CH_2Cl_2.

(P-dione)Cu **2b** is characterized by a B band at 408 nm and a weaker intensity band at 486 nm in CH_2Cl_2 solution containing 0.1 M TBAP. When a controlled potential of −0.60 V is applied to the (P-dione)Cu **2b** solution in the thin-layer cell, the B band at 408 nm increases in intensity and shifts to 412 nm as the 486 nm band disappears and is replaced by two visible bands at 536 and 570 nm. These spectral changes are shown in Figure 2a and contrast with the first reduction of (P)Cu **1b** (Figure 2d) where a porphyrin π-radical anion is produced and the B band absorption significantly decreases in intensity and the Q bands disappear, being replaced in most cases by a broad band between 600 and 900 nm. The fact that this does not occur in the case of (P-dione)Cu **2b** clearly indicates that the porphyrin macrocycle is not reduced during the first one-electron addition. The significantly small HOMO−LUMO gap of (P-dione)Cu **2b** (1.59 eV) as compared with that of (P)Cu **1b** (2.40 eV) in Table 1 also indicates that the site of the first reduction is not the porphyrin macrocycle.

A porphyrin π-radical anion or dianion UV−visible spectrum is also not obtained during the second one-electron reduction of (P-dione)Cu **2b** at an applied potential of −1.40 V. Here the 412 nm band again increases rather than decreases in intensity and shifts to 415 nm as new Q bands grow in at 505 and 541 nm. These spectral changes are illustrated in Figure 2b where the final UV−visible spectrum of the doubly reduced copper(II) porphyrin-dione resembles a porphyrin spectrum without the oxo groups in that it has a narrower and more intense B band.

Finally, during the third reduction of (P-dione)Cu **2b** at −1.70 V, the Soret band at 415 nm collapses as is expected for addition of an electron to the porphyrin π-ring system. These spectral changes are shown in Figure 2c and are similar to what is seen during the unambiguous macrocycle-centered reduction of (P)Cu **1b** (Figure 2d). The above-described spectral changes clearly indicate that the first two one-electron additions to (P-dione)Cu **2b** occur at the dione unit, while the third one-electron addition occurs exclusively at the porphyrin π-ring system. The other (P-dione)M complexes, where M = 2H, Zn, Ni, or Pd, show similar spectral changes during the three reductions, thus suggesting the same mechanism of electron transfer in each case.[62]

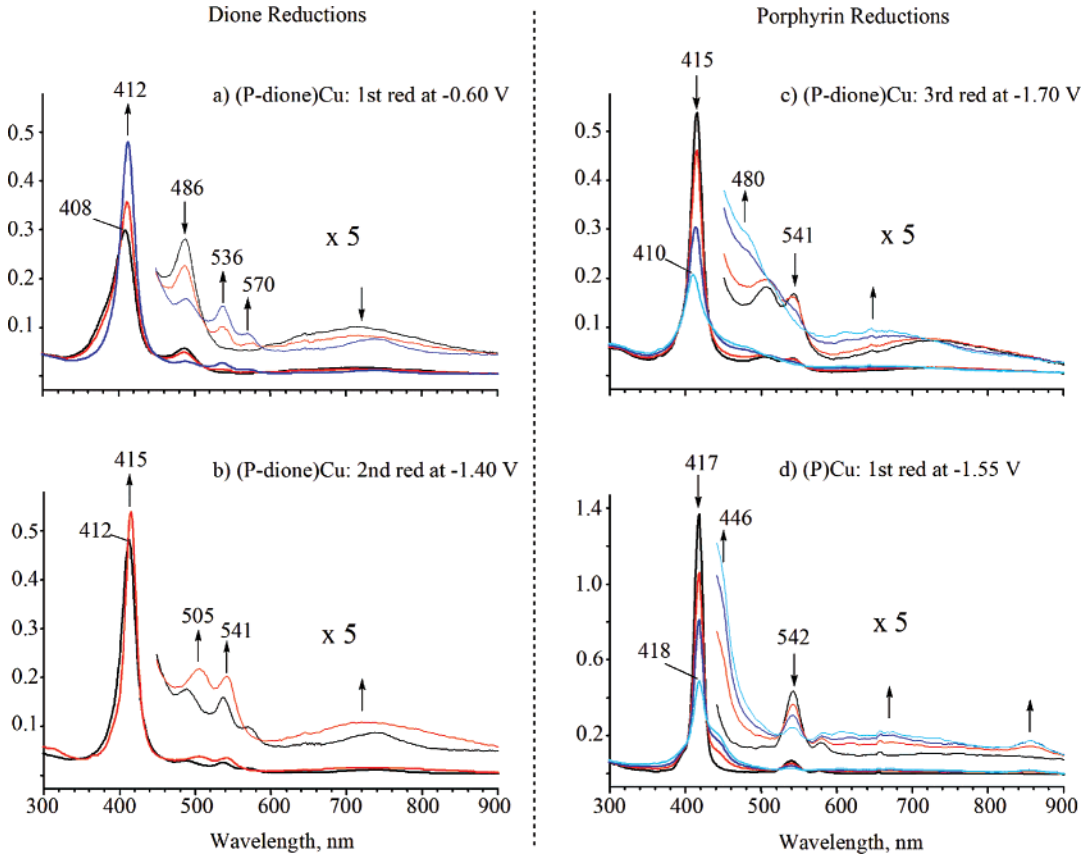

Figure 2. UV−visible spectral changes of (P-dione)Cu **2b** during (a) the first, (b) second, and (c) third reduction and (d) (P)Cu **1b** during the first reduction in CH_2Cl_2, 0.2 M TBAP.

For ESR measurements, radical anions of the porphyrin-diones were produced by photoinduced electron transfer from dimeric 1-benzyl-1,4-dihydronicotinamide $[(BNA)_2]$[63] to the (P-dione)M derivatives **2a**−**e** in MeCN as shown in Scheme 2. The $(BNA)_2$ is known to act as a unique electron donor to produce radical anions of electron acceptors.[64]

The first one-electron addition to the oxo group of porphyrin-2,3-diones was confirmed by ESR measurements (Figure 3).[65] ESR spectra for the radical anions of (P-dione)Zn **2c** and (P-dione)2H **2a** obtained under photoirradiation are shown in Figure 3. ESR spectra with hyperfine splitting due to one nitrogen are observed for both compounds, indicating that the unpaired electron is not delocalized on the porphyrin ring but rather is localized on the dione unit. The fact that the radical anion of (P-dione)2H **2a** shows no hyperfine splitting due to a proton (Figure 3b) indicates that hydrogen is not attached to the nitrogen of the pyrrolic ring which contains the dione radical anion.

The above data show that, for both free-base and metalated (P-dione)M **2a**−**e**, the dione unit is reduced and that this leads to a specific arrangement of the inner hydrogens in (P-dione)-2H **2a**. An explanation of the differences in the redox properties between the free-base and metalated porphyrins is now advanced. All free-base porphyrins are known to exist as an equilibrium mixture of "*trans*" tautomers in which the hydrogens of the inner nitrogens of the macrocycle lie on opposite pyrrolic rings and the aromatic delocalization follows an 18-atom 18 π-electron bacteriochlorin-like "inner−outer−inner−outer" pathway;[66−70] tautomers in which the hydrogens reside on adjacent "*cis*" inner nitrogens have been calculated to be of

Scheme 2

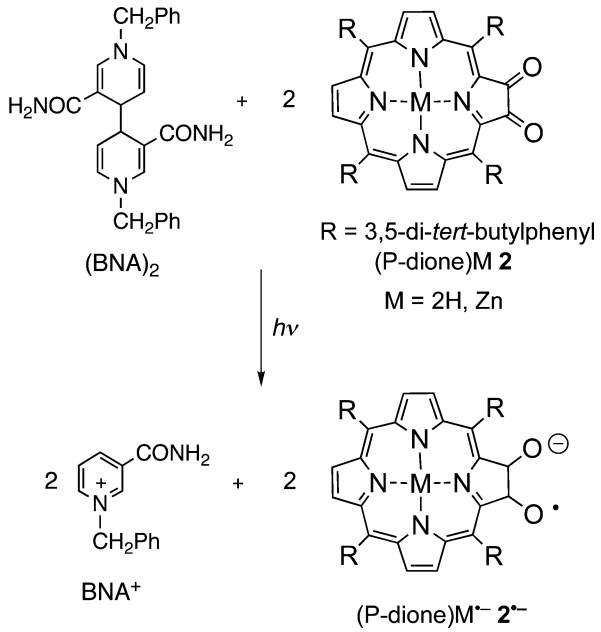

(62) For UV−visible spectral data of the neutral and reduced porphyrin-diones in CH_2Cl_2, 0.1 M TBAP, see Supporting Information S4.
(63) Patz, M.; Kuwahara, Y.; Suenobu, T.; Fukuzumi, S. *Chem. Lett.* **1997**, 567.
(64) Fukuzumi, S.; Suenobu, T.; Patz, M.; Hirasaka, T.; Itoh, S.; Fujitsuka, M.; Ito, O. *J. Am. Chem. Soc.* **1998**, *120*, 8060.
(65) The first one-electron addition to the dione group of porphyrin-2,3-dione **2a** is confirmed by thin layer FTIR spectroelectrochemical measurements showing the disappearance of the carbonyl absorption (see Supporting Information S5).

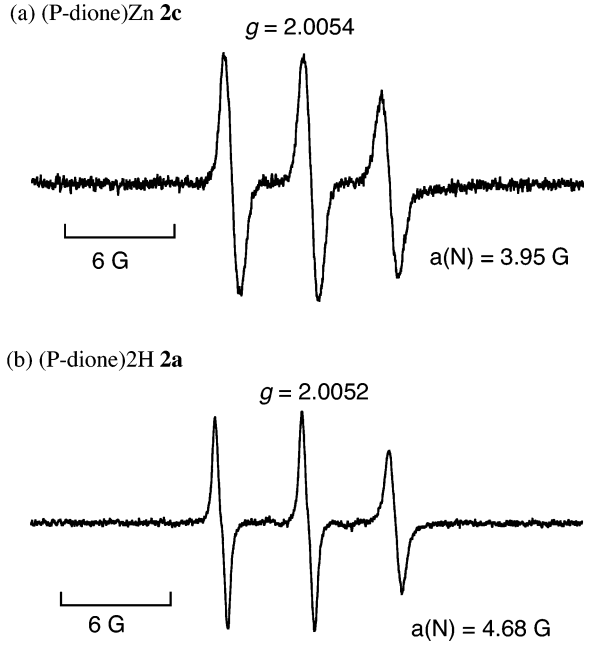

Figure 3. ESR spectra for radical anions of (a) (P-dione)Zn **2c** and (b) (P-dione)2H **2a**, produced by photoinduced electron transfer from $(BNA)_2$ (2.5×10^{-4} M) to the porphyrins (5.0×10^{-4} M) in CH_2Cl_2 at 298 K.

much higher energy[70] and are not detected by ^{1}H NMR.[66−69] Tautomers with a 17-atom 18 π-electron homologous "pyrrole-like" "inner−inner−inner−outer" aromatic pathway are also of higher energy than an 18-atom pathway.[67] In each tautomer, rings in which the inner nitrogens are not protonated have an isolated double bond between the β,β'-positions. In asymmetrically substituted porphyrins, the position of the tautomeric equilibrium is dependent on the subsituents.[66−69]

(P-dione)2H should exist as an equilibrium mixture of the forms **5a** and **5b** (Figure 4), but there is bond localization in the substituted ring caused by the dione unit which "locks" single bond character across the β,β'-positions of that ring so only one "*trans*" tautomer can show an 18-atom 18 π-electron "inner−outer−inner−outer" pathway, tautomer **5a**. In fact tautomer **5a** is the sole species detected by ^{1}H NMR of (P-dione)2H **2a** at room temperature.[16] This is also supported by the DFT calculations (UB3LYP/6-31G(d)//UBLLYP/3-21G), which indicate that **5a** is by 6.9 kcal mol^{-1} more stable than **5b**. Furthermore in the one-electron reduced species, there is what essentially is a localized semidione radical anion that again "locks" the β,β'-position bonding, this time as a double bond leading to **6**, again by destabilizing the tautomer with an inner hydrogen on the substituted ring nitrogen. For this reason no hyperfine splitting due to hydrogen is observed in the ESR spectrum of the radical anion of (P-dione)2H **2a** (Figure 3b), the species formed as **6** (Figure 4). The semidione radical anion unit is, of course, resonance stabilized itself. In this tautomer, the semidione radical anion unit is more stable than it would

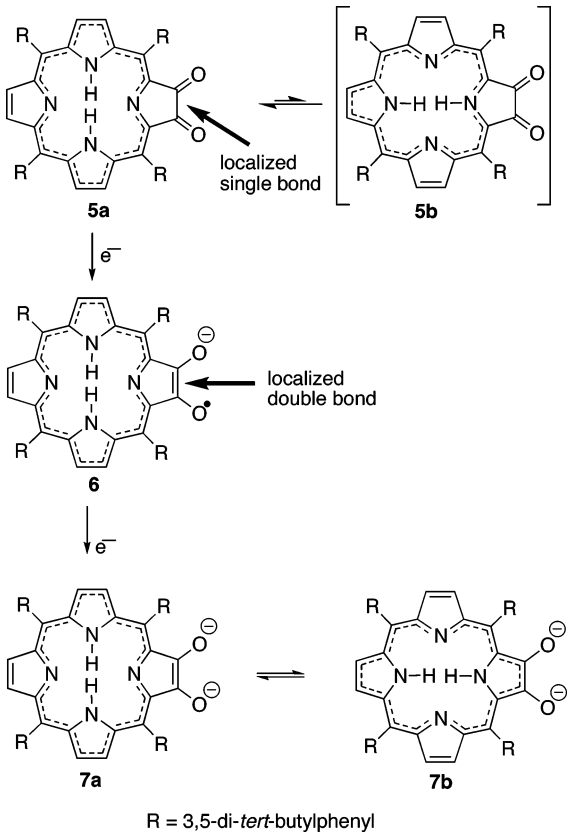

Figure 4. Tautomerism and aromatic delocalization pathways in (P-dione)-2H **2a** and its one- and two-electron reduced forms (aromatic delocalization pathways are shown as dotted lines).

be as a semiquinone radical anion and is essentially isolated, while the rest of the macrocycle is essentially neutral and retains a chlorin-like structure with an 18-atom 18 π-electron bacteriochlorin-like "inner−outer−inner−outer" pathway.

One-electron reduction of the radical anion **6** is favored because it liberates a second tautomer in the dianion product, and in this tautomer **7b** the two negatively charged oxygens sit on the aromatic pathway allowing the charge to be partially delocalized in the porphyrin structure. Although we have not determined the position of the tautomeric equilibrium in the free-base dianions, this delocalization of charge should lead to tautomer **7b** being strongly favored over tautomer **7a.** Consequently this delocalization of charge into the porphyrin ring makes the third reduction, porphyrin ring reduction, more difficult. In metalated derivatives of a symmetrical porphyrin all the bond orders across all β,β'-positions are the same.[71] There is thus less extra stabilization to be gained by disrupting the semidione radical anion, and so it remains effectively isolated in the first reduction product of (P-dione)M **2b**−**e**. An example of such isolation is seen in the one-electron reduction of cyclobutene-diones that has been reported to form an isolated semidione radical anion, because an antiaromatic compound would result if the bond was delocalized.[72] Similarly the second reduction is not promoted as much as in the free-base analogue, and the third reduction is not as destabilized.

Electrochemistry of Linear and Corner Porphyrin-Tetraones, 3 and 4. The electrochemistry of the porphyrin-tetraones

(66) Crossley, M. J.; Harding, M. M.; Sternhell, S. *J. Am. Chem. Soc*. **1986**, *108*, 3608.
(67) Crossley, M. J.; Harding, M. M.; Sternhell, S. *J. Org. Chem*. **1988**, *53*, 1132.
(68) Crossley, M. J.; Field, L. D.; Harding, M. M.; Sternhell, S. *J. Am. Chem. Soc*. **1987**, *109*, 2335.
(69) Crossley, M. J.; Harding, M. M.; Sternhell, S. *J. Org. Chem*. **1992**, *57*, 1833.
(70) Reimers, J. R.; Lü, T. X.; Crossley, M. J.; Hush, N. S. *J. Am. Chem. Soc*. **1995**, *117*, 2855.
(71) Crossley, M. J.; Harding, M. M.; Sternhell, S. *J. Am. Chem. Soc*. **1992**, *114*, 3266.
(72) Rieke, R. D.; White, C. K.; Rhyne, L. D.; Gordon, M. S.; McOmie, J. F. W.; Hacker, N. P. *J. Am. Chem. Soc*. **1977**, *99*, 5387.

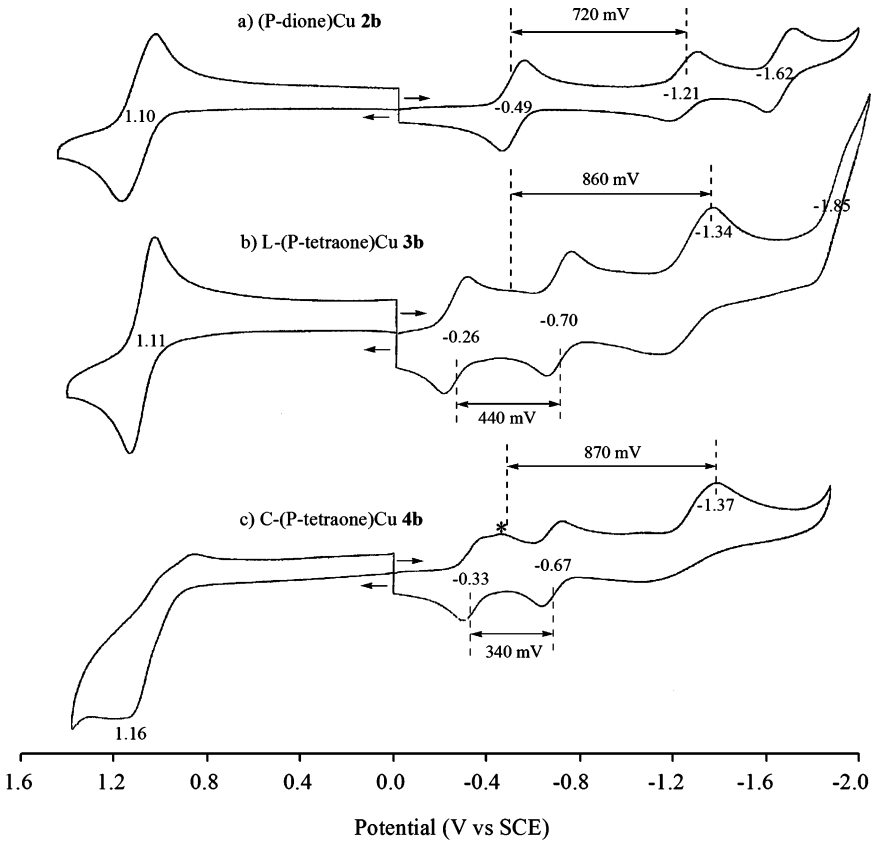

Figure 5. Cyclic voltammograms of (a) (P-dione)Cu **2b**, (b) L-(P-tetraone)Cu **3b**, and (c) C-(P-tetraone)Cu **4b** in CH_2Cl_2, 0.1 M TBAP (the peak indicated by a star is due to a side product of the first reduction).

is similar to that of the porphyrin-diones in that the first two one-electron additions occur at the easily reducible oxygen units, forming semidiones. Six electrons might be added to each porphyrin-tetraone (two at the conjugated macrocycle and one at each of the four dioxo groups), but only three or four electron additions could be observed within the negative potential limit of the utilized solvent, the remainder occurring at potentials too negative to be monitored under our experimental conditions. A summary of half-wave potentials for oxidation and reduction of the 10 investigated porphyrin-tetraones **3a**−**e** and **4a**−**e** is given in Table 1,[56] and examples of cyclic voltammograms for the Cu(II) derivatives in the two series of porphyrin-tetraones are shown in Figure 5 which also includes a cyclic voltammogram of (P-dione)Cu **2b** under the same experimental conditions.

On the basis of the combined electrochemical and spectroscopic data, the first three one-electron reductions of L-(P-tetraone)Cu **3b** and C-(P-tetraone)Cu **4b** can be unambiguously assigned as occurring at the dione unit rather than at the macrocycle. The product of the first two reductions yields a di[semidione radical anion] where a single negative charge resides on each of the two separated oxygen atoms of the compound, while the third one-electron addition then gives a trianionic species where at least three out of the four oxygen atoms on the porphyrin have been reduced prior to accessing the conjugated π-ring system of the porphyrin. These reactions are shown in Schemes 3 and 4. The site of reduction in the fourth one-electron addition could not be determined due to the proximity of this reaction to the negative potential limit of the solvent.

The electrochemistry of the porphyrin-tetraones can be interpreted in terms of a system containing two equivalent redox centers (the dione units) that interact with each other across a bridge, the bridge in this case being the conjugated porphyrin macrocycle. Under these conditions the initial formation of the semidione radical anion in the porphyrin-tetraones **3** and **4** is split into separated one electron-transfer processes; one is easier for reduction of (P-dione)M **2** with the same metal ion, and the other is harder, the absolute potential difference between the two $E_{1/2}$ values of L-(P-tetraone)M **3** and C-(P-tetraone)M **4** being a measure of the degree of interaction between the two redox centers.

The splitting of the two dione-centered redox reactions in the Cu(II) porphyrin-tetraones **3b** and **4b** is shown graphically in Figure 5 where the midpoint potential between the first and second reductions of the linear tetraone Cu **3b** ($E_{1/2} = -0.26$ and -0.70 V) and the corner tetraone Cu **4b** ($E_{1/2} = -0.33$ and -0.67 V) are -0.48 and -0.50 V, respectively in CH_2Cl_2. The average of the first two reduction potentials is -0.49 V, exactly the same $E_{1/2}$ value as that for reduction of Cu **2b**, the compound having a single dione unit on the porphyrin.

The splitting of the two dione-centered redox processes is larger for L-(P-tetraone)Cu **3b** (440 mV) than for C-(P-tetraone)-Cu **4b** (340 mV), consistent with a greater interaction between the two equivalent redox centers in the linear Cu(II) tetraone **3b** than in the corner Cu(II) tetraone **4b** and the same can be said for all metalated porphyrin-tetraones in the two series where the separation in potentials averages 403 mV between the first two reductions of L-(P-tetraone)M **3b**−**e** and 343 mV between the first two reductions of C-(P-tetraone)M **4b**−**e**.

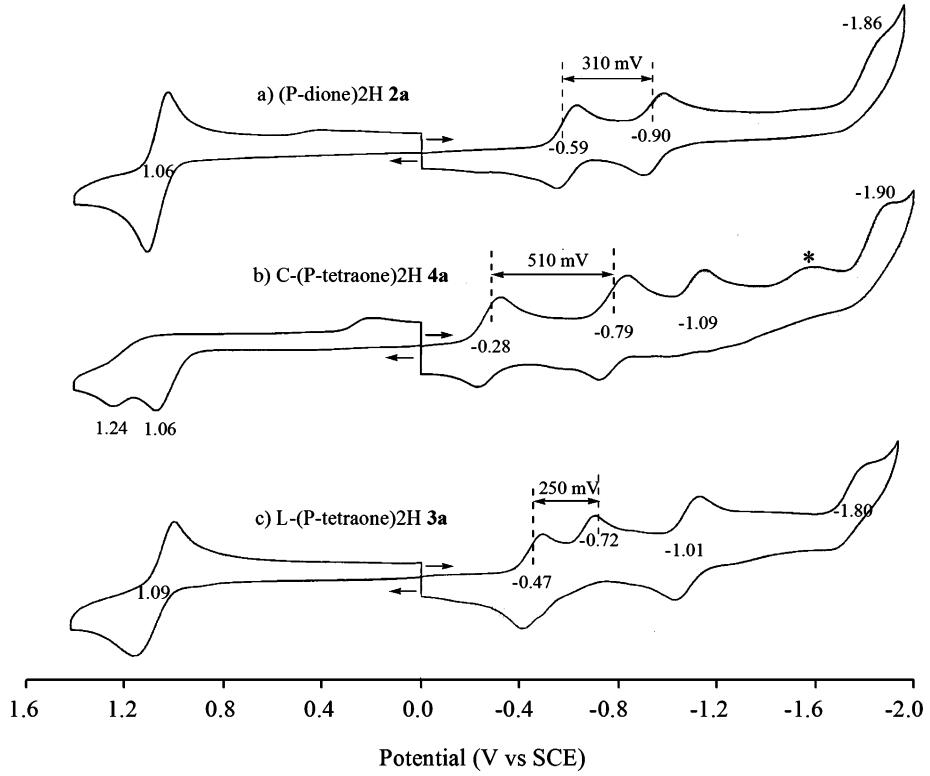

Figure 6. Cyclic voltammograms of (a) (P-dione)2H **2a**, (b) C-(P-tetraone)2H **4a**, and (c) L-(P-tetraone)2H **3a** in CH_2Cl_2, 0.1 M TBAP.

Scheme 3

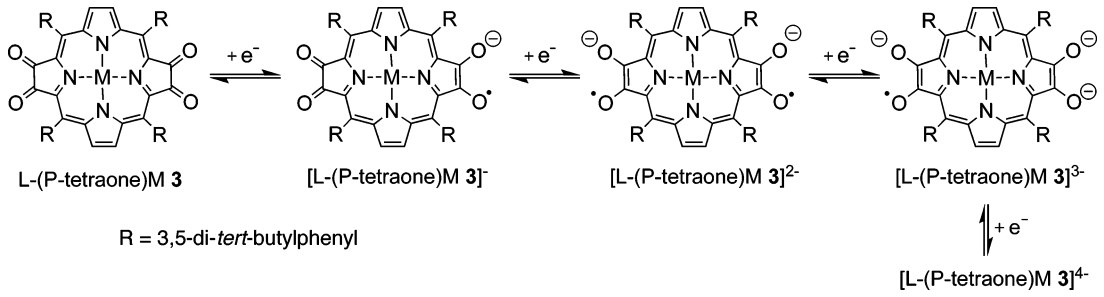

Scheme 4

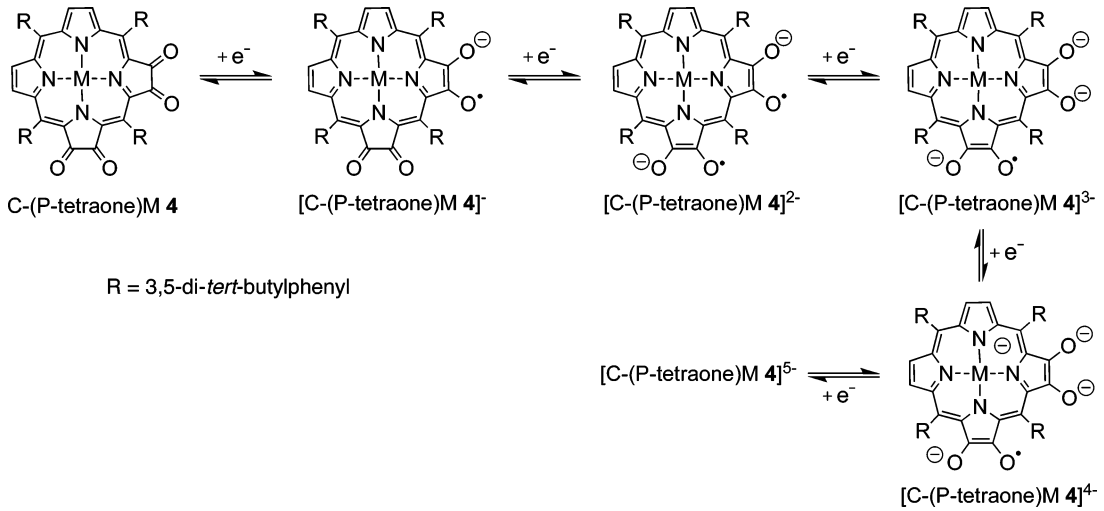

Interestingly, the splitting in potentials between the first two dione-centered redox processes of the free-base C-(P-tetraone)-2H **4a** ($E_{1/2} = -0.28$ and -0.79V) is much larger ($\Delta E_{1/2} =$ 510 mV) than that for the same reductions in the metalated series of corner porphyrin-tetraones, while the opposite is true in the case of the linear free-base L-(P-tetraone)2H **3a** where the first two reductions occur at $E_{1/2} = -0.47$ and -0.72 V giving a $\Delta E_{1/2} = 250$ mV as compared to an average 342 mV for the

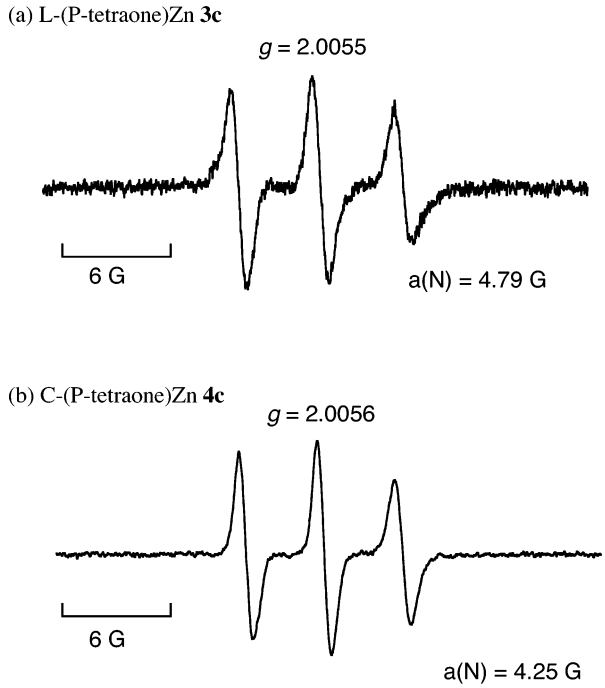

Figure 7. ESR spectra for the radical anions of (a) L-(P-tetraone)Zn **3c** and (b) C-(P-tetraone)Zn **4c** produced by photoinduced electron transfer from $(BNA)_2$ (2.5×10^{-4} M) to the porphyrins (5.0×10^{-4} M) in CH_2Cl_2 at 298 K.

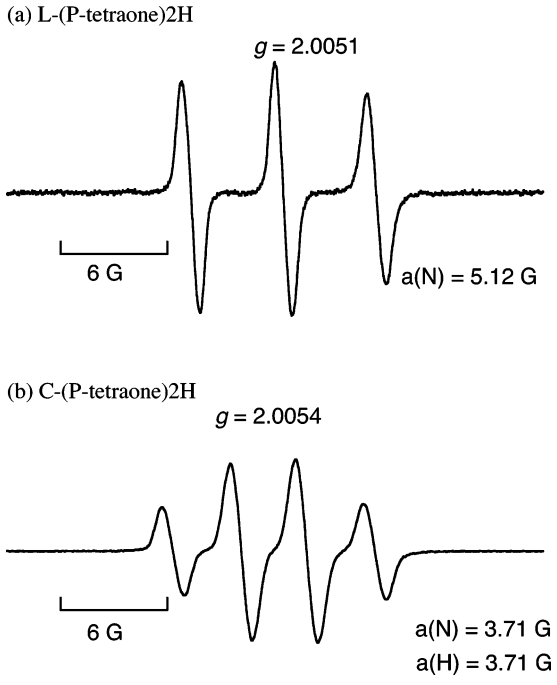

Figure 8. ESR spectra for the radical anions of (a) L-(P-tetraone)H_2 and (b) C-(P-tetraone)H_2, produced by photoinduced electron transfer from $(BNA)_2$ (2.5×10^{-4} M) to the porphyrins (5.0×10^{-4} M) in CH_2Cl_2 at 298 K.

other metalated compounds in the series (Figure 6). It is due to the first reduction of C-(P-tetraone)2H **4a** being easier as it leads to greater aromaticity (vide infra).

The spectroscopic data indicate that the third reduction of the metalated porphyrin-tetraones involves an electron addition to one of the already reduced diones, thus generating the trianionic species with an unreduced porphyrin macrocycle.[73] The third electrode reaction is easier for the L-(P-tetraones)M **3b**−**e** than for the C(P-tetraones)M **4b**−**e** derivatives by an average of 120 mV in CH_2Cl_2 (see Table 1). In addition, the separation between the second and third reductions is close to 700 mV, about the same potential separation observed between the first and second reductions of the metalated porphyrin-diones where the second electron goes onto an adjacent already-reduced oxygen atom.

The site of the first one-electron addition to a dione group of porphyrin-tetraones was also confirmed by ESR measurements. In the case of the radical anions of L-(P-tetraone)Zn **3c** and C-(P-tetraone)Zn **4c** (Figure 7), the ESR spectra exhibit hyperfine splitting due to only one nitrogen, indicating that the unpaired electron is localized on only a single dione unit of the porphyrin-tetraone.

In the case of the radical anion of C-(P-tetraone)2H **4a**, there is additional hyperfine splitting due to one proton, whereas no hyperfine splitting due to the proton is observed for the radical anion of L-(P-tetraone)2H **3a** (Figure 8). There must be in the case of C-(P-tetraone)2H a hydrogen attached to one of the pyrrolic ring nitrogens containing the semidione radical anion unit. A substantially easier first reduction of C-(P-tetraone)2H **4a** is seen in both solvents ($E_{1/2} = -0.28$ V in CH_2Cl_2 and -0.26 V in PhCN).

(73) For UV−visible spectral data of the neutral and one-, two-, three-, and four-electron reduced porphyrin-tetraones in CH_2Cl_2, 0.1 M TBAP, see Supporting Information S6 (L-(P-tetraone)Ni **3d**) and S7 (C-(P-tetraone)-Ni **4d**).

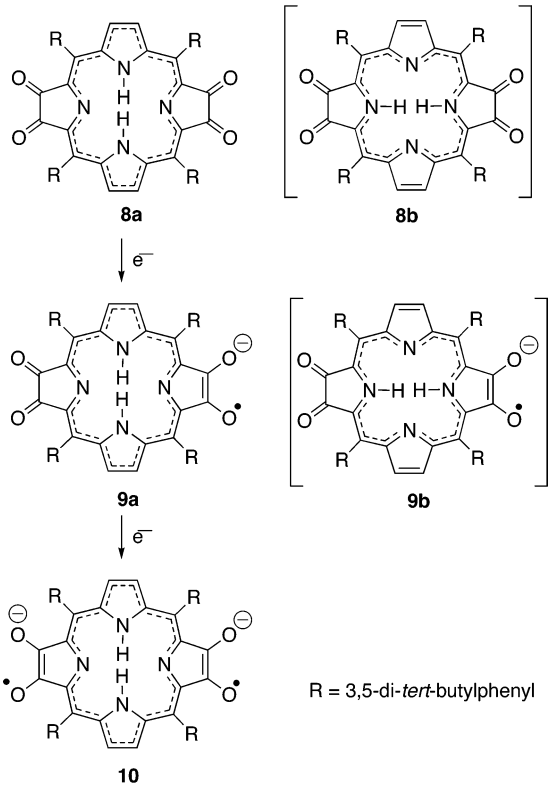

Figure 9. Tautomerism and aromatic delocalization pathways in L-(P-tetraone)2H **3a** and its one- and two-electron reduced forms (aromatic delocalization pathways are shown as dotted lines).

The relative ease in the first reduction of C-(P-tetraone) **4a** can be understood in terms of the effect of reduction on the tautomeric processes that operate in the free-base porphyrin-tetraones **3a** (Figure 9) and **4a** (Figure 10). Linear porphyrin-tetraone **3a** exists as the tautomer **8a** as is readily discerned

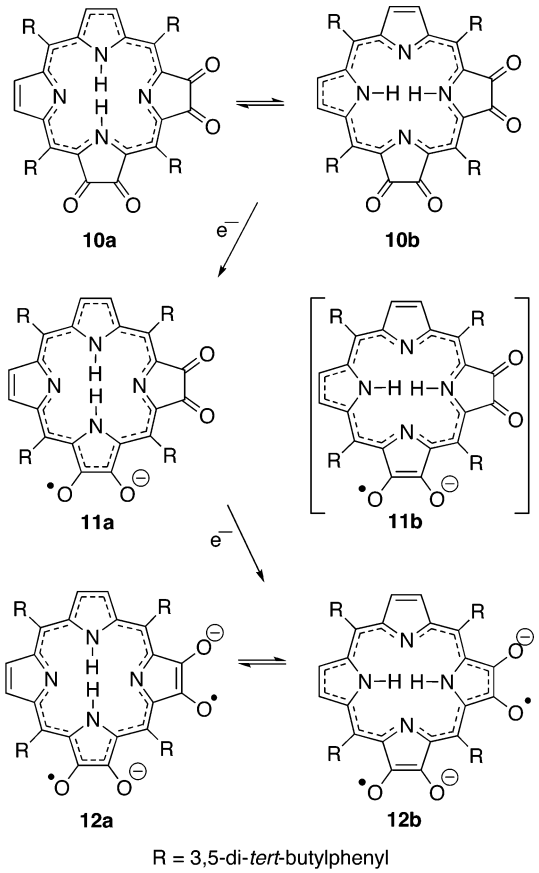

Figure 10. Tautomerism and aromatic delocalization pathways in C-(P-tetraone)2H **4a** and its one- and two-electron reduced forms (aromatic delocalization pathways are shown as dotted lines).

from the ^{1}H NMR spectrum in $CDCl_3$ where the four equivalent β-pyrrolic protons resonate as a doublet (^4J = 1.8 Hz) at 8.50 ppm that collapses to a singlet upon irradiation of the two-proton broad singlet (N−H) at −1.80 ppm. This compound has a striking visible spectrum with a blue-shifted B band at 386 nm and a red-shifted Q_y band at 772 nm and resembles that of a bacteriochlorin which has a locked 18-atom 18 π-electron aromatic delocalization pathway.[16] The alternate tautomer **8b** has a very unfavorable 16-atom 18 π-electron aromatic delocalization pathway (Figure 9). The DFT calculations (UB3LYP/6-31G(d)//UB3LYP/3-21G) indicate that **8a** is by 18.1 kcal mol^{-1} more stable than **8b**.

The first reduction gives **9a** in which the electron has reduced a dione unit which remains isolated from the 18-atom 18 π-electron aromatic delocalization pathway; tautomer **9b** is very unfavorable as before. The DFT calculations indicate that **9a** is by 5.2 kcal mol^{-1} more stable than **9b**. The second reduction gives **10** on electrostatic grounds as there is no advantage in reducing the first semidione radical anion unit further, as at best it could create an alternate 17-atom 18 π-electron aromatic delocalization pathway having much higher energy than **10**. The third reduction also takes place on the peripheral unit for the same reason.

In the case of the corner tetraone, C-(P-tetraone) **4a**, the first example of tautomerism being "switched off", here by a reversible one-electron process, is observed (Figure 10).

Corner tetraone C-(P-tetraone) **4a** exists as a 1:1 mixture of the degenerate tautomers **10a** and **10b**. The aromatic delocalization of these tautomers necessarily involves a relatively higher energy "inner−inner−inner−outer" 17-atom 18 π-electron pathway. One-electron reduction leads to the tautomer **11a** being formed as the overwhelmingly dominant product, thereby "turning off" the tautomeric reaction and creating a new, more stable "outer−inner−outer−inner" 18-atom 18 π-electron aromatic pathway (Figure 10). This tautomer, with an inner hydrogen on the nitrogen of the ring at which electron-transfer occurred, is detected by ESR (Figure 8b), and the energy gained is reflected in it being the easiest of the compounds in this study to be reduced by one electron. The alternate tautomer **11b** still has a higher energy "inner−inner−inner−outer" 17-atom 18 π-electron pathway. The second reduction gives the degenerate tautomers **12a** and **12b** and turns the tautomeric process "on" again. The only previous example of such a switching off of tautomerism was observed in a complex system involving the compound 2-hydroxy-5,10,15,20-tetraphenylporphyrin where a secondary enol-keto tautomerism leads to a 5:3:2 equilibrium mixture of essentially a single tautomer of the keto form and two tautomers of the enolic hydroxy form.[67] The present case of C-(P-tetraone)2H **4a** is the only case of the process leading to essentially a single entity.

Conclusions

In contrast to porphyrins that exhibit two one-electron reductions, three one-electron reductions are observed for reduction of the porphyrin-2,3-diones. The electrochemical, UV−visible spectroelectrochemical, and ESR data indicate that the first two one-electron reductions involve the oxo groups of the dione unit, followed by the third reduction on the porphyrin ring at more negative potentials. In the case of porphyrin-2,3,7,8-tetraones and porphyrin-2,3,12,13-tetraones, the first three one-electron reductions occur at dione units prior to accessing the conjugated π-ring system of the porphyrin. Thus, the dione unit, while involving carbons that are part of the porphyrin macrocyclic framework, can show *independent redox chemistry* from that of the porphyrin ring. Such unique redox properties of porphyrin-diones and -tetraones will make it possible to vary the reduction potentials more significantly by binding of metal ions to the dione units without changing the oxidation potentials. This will certainly expand the scope of electron-transfer chemistry of porphyrins. One-electron reduction of the corner tetraone C-(P-tetraone)2H **4a** causes an unprecedented "locking" of the tautomeric inner hydrogen exchange process.

Experimental Section

General. Microanalyses were performed by the Campbell Microanalytical Laboratory, University of Otago, New Zealand. Infrared spectra were recorded on a Perkin-Elmer model 1600 FT-IR spectrophotometer and on Fourier transform infrared spectrophotometer FTIR-8400S SHIMADZU of solutions in the stated solvents. Ultraviolet−visible spectra were routinely recorded on a Cary 5E UV−vis−NIR spectrophotometer in chloroform that was deacidified by filtration through an alumina column. ^{1}H NMR spectra were recorded on either a Bruker AC-200 (200 MHz) or a Bruker DPX-400 (400 MHz) spectrometer as stated. Samples were dissolved in deuteriochloroform ($CDCl_3$), and the chloroform peak at 7.26 ppm was used as an internal reference unless otherwise stated. Deuterated solvents were used as received except for deuterated chloroform, which was deacidified by filtration through a plug of alumina.

Matrix assisted laser desorption ionization time-of-flight (MALDI-TOF) mass spectra were recorded on a VG TofSpec spectrometer. For all the porphyrin derivatives described in this paper no matrix was

required. Mass spectra were obtained as an envelope of the isotope peaks of the molecular ion. The mass corresponding to the maxima of the envelope is reported and was compared with the maxima of a simulated spectrum. Electrospray ionization (ESI) and atmospheric pressure chemical ionization (APCI) mass spectra were recorded on a ThermoQuest Finnigan LCQ DECA instrument. High-resolution electrospray ionization Fourier transform ion cyclotron resonance (HR-ESI-FT/ICR) spectra were either acquired at the School of Chemistry, The University of New South Wales on a Bruker Daltonics BioAPEX II FT/ICR mass spectrometer equipped with a 7 T MAGNEX superconducting magnet and an Analytica external ESI source or acquired at the Research School of Chemistry, Australian National University on a Bruker Daltonics BioAPEX II FT/ICR mass spectrometer equipped with a 4.7 T MAGNEX superconducting magnet and an Analytica external ESI source. Electrospray ionization high-resolution mass spectrometry (ESI-HRMS) data were either recorded on a VG Quattro II triple quadrupole mass spectrometer at the Research School of Chemistry, Australian National University or recorded on a Finnigan MAT 900 × L mass spectrometer at the School of Molecular and Microbial Sciences, The University of Queensland.

All commercial solvents were routinely distilled prior to use. Solvent mixture proportions are given by volume ratios. Light petroleum refers to the fraction with bp 60−80 °C.

Electrochemical Measurements. Absolute dichloromethane (CH_2Cl_2) and pyridine were received from Aldrich Co. and used as received without further purification. Tetra-*n*-butylammonium perchlorate (TBAP) was purchased from Sigma Chemical or Fluka Chemika Co., recrystallized from ethyl alcohol, and dried under vacuum at 40 °C for at lease 1 week prior to use.

Cyclic voltammetry was carried out by using an EG&G Princeton Applied Research (PAR) 173 potentiostat/galvanostat. A homemade three-electrode cell was used for cyclic voltammetric measurement and consisted of a platinum button or glassy carbon working electrode, a platinum counter electrode, and a homemade saturated calomel reference electrode (SCE). The SCE was separated from the bulk of the solution by a fritted glass bridge of low porosity, which contained the solvent/Supporting electrolyte mixture. UV−visible spectroelectrochemical experiments were performed with a home-built thin-layer cell that had a light transparent platinum net working electrode. Potentials were applied and monitored with an EG&G PAR model 173 potentiostat. Time-resolved UV−visible spectra were recorded with a Hewlett-Packard model 8453 diode array spectrophotometer. Thin-layer FTIR spectroelectrochemical measurements were carried out with an FTIR Nicolet 550 Magna-IR spectrometer using a specially constructed light transparent FTIR spectroelectrochemical cell.

ESR Measurements. Semidione radical anions were prepared by the photoreduction of porphyrin-diones and porphyrin-tetraones with $(BNA)_2$ in deaerated MeCN. Typically, a porphyrin dione was dissolved in CH_2Cl_2 (5.0×10^{-4} M in 300 μL) containing $(BNA)_2$ (2.5×10^{-4} M) and purged with argon for 10 min. The solution was bubbled with Ar gas through a syringe that has a long needle. ESR spectra were recorded on a JEOL JES-RE1XE spectrometer under irradiation of a high-pressure mercury lamp (USH-1005D) by focusing at the sample cell in the ESR cavity at 298 K. Semidione radical anions were also produced by the electron-transfer reduction of porphyrin-diones and porphyrin-tetraones by a tetramethyl-*p*-benzosemiquinone radical anion ($Me_4Q^{\bullet -}$) in CH_2Cl_2. The magnitude of modulation was chosen to optimize the resolution and signal-to-noise (*S*/*N*) ratio of the observed spectra under nonsaturating microwave power conditions. The *g* values were calibrated using a Mn^{2+} marker.

Synthesis. Unless stated otherwise, new compounds were crystallized from a chloroform−acetonitrile solution. Synthesis of porphyrin-diones **2a**−**d** and linear porphyrin-tetraones **3a,b** have been described earlier.[16−18,29,30]

{**2,3-Dioxo-5,10,15,20-tetrakis(3,5-di-*tert*-butylphenyl)chlorinato**}-**palladium(II) (2e).** Dione **2a** (22.5 mg, 0.0206 mmol), palladium(II) chloride (32.0 mg, 0.180 mmol), and sodium acetate (46.0 mg, 0.561 mmol) were dissolved in toluene (8 mL) and glacial acetic acid (18 M, 8 mL), and the mixture was heated at reflux for 2 min. Dichloromethane (30 mL) was added to the mixture, and the organic phase was separated; washed with water (200 mL), sodium carbonate solution (10%, 150 mL), and water (200 mL); dried over anhydrous sodium sulfate; and filtered, and the filtrate was evaporated to dryness. The product was purified by column chromatography over silica (CH_2Cl_2−light petroleum; 1:1). The front running green band afforded **2e** (24.5 mg, 99%) as a green microcrystalline solid, mp >300 °C. IR ($CHCl_3$): 2965s, 2869m, 1724s, 1593s, 1477m, 1364s, 1300m, 1108m, 1020w cm^{-1}. UV−vis ($CHCl_3$): 269 (log ϵ 4.35), 404 (5.16), 478 (4.34), 611 (3.72), 683 (3.73) nm. ^{1}H NMR (400 MHz, $CDCl_3$): δ 1.44 (36 H, s, *tert*-butyl H); 1.47 (36 H, s, *tert*-butyl H); 7.58 (4 H, d, *J* 1.8 Hz, H_o); 7.69 (2 H, t, *J* 1.7 Hz, H_p); 7.73 (2 H, t, *J* 1.8 Hz, H_p); 7.86 (4 H, d, *J* 1.8 Hz, H_o); 8.22 (2 H, d, *J* 5.1 Hz, β-pyrrolic H); 8.46 (2 H, d, *J* 5.1 Hz, β-pyrrolic H); 8.50 (2 H, s, β-pyrrolic H). MS (ESI) (*m*/*z*): 1197.6 (M^+ requires 1198.0). HR-ESI-FT/ICR Found: $[M + H]^+$ 1197.6166. $C_{76}H_{90}N_4O_2Pd$ requires 1197.6196.

{**2,3,12,13-Tetraoxo-5,10,15,20-tetrakis(3,5-di-*tert*-butylphenyl)-bacteriochlorinato**}**zinc(II) (3c).** Tetraone **3a** (13.2 mg, 0.0117 mmol) and zinc(II) acetate dihydrate (100 mg, 0.456 mmol) in chloroform (12 mL) and methanol (6 mL) was heated at reflux for 52 h. The solvent was removed under vacuum, and the residue was purified by column chromatography over silica (CH_2Cl_2). The major green band was collected, and the solvent was removed to afford **3c** (7.6 mg, 55%) as a green microcrystalline solid, mp >300 °C. Found: C, 73.01; H, 7.33; N, 4.56. $C_{76}H_{88}N_4O_4Zn + {}^1/_2CH_3CN + {}^1/_2CHCl_3$ requires C, 73.46; H, 7.16; N, 4.97%. IR ($CHCl_3$): 3061w, 2964s, 2905m, 2868m, 1717s, 1593s, 1477m, 1464w, 1429w, 1394m, 1364m, 1348w, 1298w, 1265w, 1248m, 1204w, 1126w, 1078m, 1034m, 1016w cm^{-1}. UV−vis ($CHCl_3$): 398 (log ϵ 5.08), 424sh (4.74), 465sh (4.41), 546sh (3.46), 582 (3.52), 674sh (3.74), 750sh (3.90), 829 (3.93) nm. ^{1}H NMR (400 MHz, $CDCl_3$): δ 1.43 (72 H, s, *tert*-butyl H); 7.56 (8 H, d, *J* 1.8 Hz, H_o); 7.69 (4 H, t, *J* 1.8 Hz, H_p); 8.24 (4 H, s, β-pyrrolic H). MS (ESI) (*m*/*z*): 1187.5 (M^+ requires 1186.9). MS (MALDI-TOF) (*m*/*z*): 1186.4 (M^+ requires 1186.9).

{**2,3,12,13-Tetraoxo-5,10,15,20-tetrakis(3,5-di-*tert*-butylphenyl)-bacteriochlorinato**}**nickel(II) (3d).** Tetraone **3a** (62.9 mg, 0.0560 mmol), nickel(II) acetate dihydrate (300 mg, 1.410 mmol), and sodium acetate (200 mg, 2.438 mmol) were dissolved in toluene (13 mL) and glacial acetic acid (18 M, 13 mL), and the mixture was heated at reflux for 48 h. Workup was as that above, and column chromatography over silica (CH_2Cl_2−light petroleum; 1:1) gave **3d** (19.9 mg, 30%) as a green microcrystalline solid, mp >300 °C. IR ($CHCl_3$): 2964s, 2905m, 2868m 1717s, 1593m, 1541w, 1477w, 1464w, 1431w, 1408w, 1394w, 1364m, 1356m, 1302w, 1271w, 1248w, 1121w, 1084w, 1041m, 1026w, 1018w cm^{-1}. UV−vis ($CHCl_3$): 327sh (log ϵ 4.44), 373 (4.76), 397 (4.76), 464 (4.31), 492sh (4.08), 588sh (3.41), 642sh (3.63), 712 (3.87), 874sh (3.75), 949 (3.91) nm. ^{1}H NMR (400 MHz, $CDCl_3$): δ 1.38 (72 H, s, *tert*-butyl H); 7.30 (8 H, d, *J* 1.7 Hz, H_o); 7.59 (4 H, t, *J* 1.7 Hz, H_p); 8.14 (4 H, s, β-pyrrolic H). MS (ESI) (*m*/*z*): 1180.8 (M^+ requires 1180.2). ESI-HRMS Found: $[M + Na]^+$ 1201.607. $C_{76}H_{88}N_4NiO_4$ + Na requires 1201.605. The second brown band was collected, and the solvent was removed to afford unreacted **3a** (22 mg, 35%).

{**2,3,12,13-Tetraoxo-5,10,15,20-tetrakis(3,5-di-*tert*-butylphenyl)-bacteriochlorinato**}**palladium(II) (3e).** Tetraone **3a** (60.0 mg, 0.0530 mmol), palladium(II) chloride (64.0 mg, 0.361 mmol), and sodium acetate (110 mg, 1.341 mmol) were dissolved in toluene (13 mL) and glacial acetic acid (18 M, 13 mL), and the mixture was heated at reflux for 5 min. Workup was as that above, and column chromatography over silica (CH_2Cl_2−light petroleum; 1:1) gave **3e** (58.4 mg, 90%) as a green microcrystalline solid, mp >300 °C. IR ($CHCl_3$): 2964s, 2905m, 2868m, 1720s, 1593m, 1477w, 1464w, 1414w, 1394w, 1364m, 1354m, 1302w, 1248w, 1121w, 1097w, 1045s, 1030w, 1020w cm^{-1}. UV−vis ($CHCl_3$): 308sh (log ϵ 4.40), 362sh (4.64), 386 (4.83), 448

(4.46), 479sh (4.15), 581sh (3.50), 641 (3.91), 805sh (3.87), 868 (4.02) nm. ^{1}H NMR (400 MHz, $CDCl_3$): δ 1.40 (72 H, s, *tert*-butyl H); 7.44 (8 H, d, *J* 1.8 Hz, H_o); 7.65 (4 H, t, *J* 1.8 Hz, H_p); 7.99 (4 H, s, β-pyrrolic H). MS (ESI) (*m*/*z*): 1228.5 (M^+ requires 1228.0). MS (MALDI-TOF) (*m*/*z*): 1228.3 (M^+ requires 1228.0). ESI-HRMS Found: $[M + Na]^+$ 1249.575. $C_{76}H_{88}N_4O_2Pd + Na$ requires 1249.576.

{**2,3,7,8-Tetraoxo-5,10,15,20-tetrakis(3,5-di-*tert*-butylphenyl)-isobacteriochlorinato**}**copper(II) (4b).** Tetraone **4a** (20.0 mg, 0.0178 mmol) and copper(II) acetate monohydrate (40.0 mg, 0.200 mmol) in chloroform (12 mL) and methanol (6 mL) were heated at reflux for 2 min. The solvent was removed under vacuum, and the product was purified by column chromatography over silica (CH_2Cl_2−light petroleum; 1:1). The major green band afforded **4b** (18.0 mg, 85%) as a green microcrystalline solid, mp >300 °C. Found: C, 76.8; H, 7.7; N, 4.5. $C_{76}H_{88}N_4CuO_4$ requires C, 77.0; H, 7.5; N, 4.7%. IR ($CHCl_3$): 2965s, 2868w, 1724s, 1594m, 1540w, 1476w, 1364m, 1346m, 1296w, 1265w, 1218s, 1214s cm^{-1}. UV−vis ($CHCl_3$): 389 (log ϵ 4.87), 411sh (4.69), 447sh (4.37), 473 (4.43), 552 (4.05), 597 (4.05) nm. MS (MALDI-TOF) (*m*/*z*): 1185 (M^+ requires 1185). MS (ESI) (*m*/*z*): 1185.5 (M^+ requires 1185.1).

{**2,3,7,8-Tetraoxo-5,10,15,20-tetrakis(3,5-di-*tert*-butylphenyl)-isobacteriochlorinato**}**zinc(II) (4c).** Tetraone **4a** (52.0 mg, 0.0463 mmol) and zinc(II) acetate dihydrate (34.0 mg, 0.155 mmol) in chloroform (20 mL) and methanol (10 mL) were heated at reflux for 3 min. The solvent was removed under vacuum, and the residue was purified by column chromatography over silica (CH_2Cl_2). The major green band afforded **4c** (54.5 mg, 99%) as a green microcrystalline solid, mp >300 °C (from CH_2Cl_2−light petroleum). Found: C, 74.7; H, 7.4; N, 4.5. $C_{76}H_{88}N_4O_4Zn + {}^1/_2CH_2Cl_2$ requires C, 74.7; H, 7.3; N, 4.5%. IR ($CHCl_3$): 2964s, 2905m, 2868m, 1722s, 1593s, 1526w, 1477m, 1464w, 1364m, 1342m, 1294m, 1248w, 1101w, 1072w cm^{-1}. UV−vis ($CHCl_3$): 396 (log ϵ 4.94), 423sh (4.75), 457sh (4.43), 479sh (4.22), 545sh (4.10), 606 (4.04), 644sh (3.95), 724sh (3.71) nm. ^{1}H NMR (400 MHz, $CDCl_3$): δ 1.39 (18 H, s, *tert*-butyl H); 1.42 (36 H, s, *tert*-butyl H); 1.45 (18 H, s, *tert*-butyl H); 7.25 (2 H, d, *J* 1.2 Hz, H_o); 7.47 (4 H, d, *J* 1.2 Hz, H_o); 7.61 (1 H, t, *J* 1.2 Hz, H_p); 7.65 (2 H, t, *J* 1.2 Hz, H_p); 7.70 (1 H, t, *J* 1.2 Hz, H_p); 7.75 (2 H, d, *J* 1.2 Hz, H_o); 7.85 and 8.12 (4 H, ABq, *J* 4.6 Hz, β-pyrrolic H). MS (ESI) (*m*/*z*): 1186.6 (M^+ requires 1186.9).

{**2,3,7,8-Tetraoxo-5,10,15,20-tetrakis(3,5-di-*tert*-butylphenyl)-isobacteriochlorinato**}**nickel(II) (4d).** Tetraone **4a** (18.0 mg, 0.0160 mmol) and nickel(II) acetate dihydrate (40.0 mg, 0.188 mmol) were dissolved in toluene (8 mL) and glacial acetic acid (18 M, 8 mL), and the mixture was heated at reflux for 2 min. Workup was as that above, and column chromatography over silica (CH_2Cl_2−light petroleum; 1:1) afforded **4d** (18.5 mg, 98%) as a green microcrystalline solid, mp >300 °C. Found: C, 77.1; H, 7.6; N, 4.5. $C_{76}H_{88}N_4O_4Ni$ requires C, 77.3; H, 7.5; N, 4.7%. IR ($CHCl_3$): 2950s, 2919s, 2857s, 1721m, 1459m, 1377w, 1351w, 1295w, 1218s cm^{-1}. UV−vis ($CHCl_3$): 333sh (log ϵ 4.49), 399 (4.66), 476 (4.26), 571 (3.82), 599 (3.83) nm. ^{1}H NMR (400 MHz, $CDCl_3$): δ 1.31 (18 H, s, *tert*-butyl H); 1.36 (36 H, s, *tert*-butyl H); 1.41 (18 H, s, *tert*-butyl H); 6.95 (2 H, d, *J* 1.8 Hz, H_o); 7.26 (4 H, d, *J* 1.8 Hz, H_o); 7.49 (1 H, t, *J* 1.8 Hz, H_p); 7.56 (2 H, t, *J* 1.8 Hz, H_p); 7.58 (1 H, d, *J* 1.8 Hz, H_o); 7.64 (2 H, t, *J* 1.8 Hz, H_p); 7.78 and 7.97 (4 H, ABq, *J* 4.8 Hz, β-pyrrolic H). MS (MALDI-TOF) (*m*/*z*): 1181 (M^+ requires 1180). MS (ESI) (*m*/*z*): 1180.5 (M^+ requires 1180.2).

{**2,3,7,8-Tetraoxo-5,10,15,20-tetrakis(3,5-di-*tert*-butylphenyl)-isobacteriochlorinato**}**palladium(II) (4e).** Tetraone **4a** (55.8 mg, 0.0497 mmol), palladium(II) chloride (43.0 mg, 0.243 mmol), and sodium acetate (61 mg, 0.744 mmol) were dissolved in toluene (7 mL) and glacial acetic acid (18 M, 7 mL), and the mixture was heated at reflux for 3 min. Workup was as that above, and column chromatography over silica (CH_2Cl_2−light petroleum; 1:1) gave **4e** (60.5 mg, 99%) as a green microcrystalline solid, mp >300 °C. Found: C, 74.3; H, 7.3; N, 4.3. $C_{76}H_{88}N_4O_4Pd$ requires C, 74.3; H, 7.2; N, 4.6%. IR ($CHCl_3$): 2965s, 2905m, 2868w, 1723s, 1594m, 1546w, 1477w, 1363m, 1351m, 1300w, 1247w, 1215s, 1183w, 1111w, 1080w cm^{-1}. UV−vis ($CHCl_3$): 385 (log ϵ 4.99), 444 (4.40), 467 (4.46), 545sh (3.99), 579 (4.07), 718 (4.72) nm. ^{1}H NMR (400 MHz, $CDCl_3$): δ 1.39 (18 H, s, *tert*-butyl H); 1.42 (36 H, s, *tert*-butyl H); 1.46 (18 H, s, *tert*-butyl H); 7.23 (2 H, d, *J* 1.8 Hz, H_o); 7.45 (4 H, d, *J* 1.8 Hz, H_o); 7.64 (1 H, t, *J* 1.8 Hz, H_p); 7.67 (2 H, t, *J* 1.8 Hz, H_p); 7.71−7.74 (3 H, m, H_o, H_p); 7.96 and 8.19 (4 H, ABq, *J* 4.9 Hz, β-pyrrolic H). MS (MALDI-TOF) (*m*/*z*): 1229 (M^+ requires 1228). MS (ESI) (*m*/*z*): 1228.7 (M^+ requires 1228.0).

Acknowledgment. The support of the Robert A. Welch Foundation (KMK, Grant E-680) and the Texas Advanced Research program to K.M.K. under Grant No. 003652-0018-2001 are gratefully acknowledged. This work was also partially supported by a Discovery Research Grant (DP0208776) to M.J.C. from the Australian Research Council and a Grant-in-Aid (No. 17750039) to K.O. from the Ministry of Education, Culture, Sports, Science and Technology, Japan.

Supporting Information Available: Table S1: Half-wave potentials (V vs SCE) of porphyrin-diones and -tetraones in PhCN, 0.1 M TBAP. Figure S1: Cyclic voltammograms of (a) (P-dione)Ni **2d**, (b) (P-dione)Zn **2c**, and (c) (P-dione)Pd **2e** in CH_2Cl_2, 0.1 M TBAP. Table S2: UV−visible spectral data of neutral and reduced porphyrin-diones in CH_2Cl_2, 0.1 M TBAP. Figure S2: Thin-layer FTIR (a) spectra of (P-dione)2H **2a** before reduction in a thin-layer FTIR cell and (b) differential spectral changes during the first reduction at −0.70 V in CH_2Cl_2, 0.2 M TBAP. Figure S3: UV−visible spectral changes of L-(P-tetraone)Ni **3d** during the (a) first, (b) second, (c) third, and (d) fourth reduction in CH_2Cl_2, 0.2 M TBAP. Figure S4: UV−visible spectral changes of C-(P-tetraone)Ni **4d** during the (a) first, (b) second, (c) third, and (d) fourth reduction in PhCN, 0.2 M TBAP. This material is available free of charge via the Internet at http://pubs.acs.org.

JA070759B